MDPI

Article

Analysis of the Influence of Temperature on the Anaerobic Digestion Process in a Plug Flow Reactor

Francesco Calise , **Francesco Liberato Cappiello** , **Luca Cimmino *** , **Marialuisa Napolitano** and **Maria Vicidomini**

Department of Industrial Engineering, University of Naples Federico II, 80125 Naples, Italy; frcalise@unina.it (F.C.); francescoliberato.cappiello@unina.it (F.L.C.); marialuisa.napolitano2@unina.it (M.N.); maria.vicidomini@unina.it (M.V.)

* Correspondence: luca.cimmino@unina.it

Abstract: The production of biogas by means of the anaerobic digestion process is becoming increasingly attractive in the green economy context. When municipal organic waste is used to produce biogas, a further positive effect on urban waste disposal is obtained. Starting from the anaerobic digestion model n.1, an accurate analysis of the temperature effects on the anaerobic digestion process in a plug flow reactor is performed. This paper aims at presenting a comprehensive and integrated one-dimensional biological and thermal model for a plug flow reactor. Partial differential equations with respect to time and space are considered to model the heat transfer between the reactor and the internal heat exchanger and between the reactor and the environment. In this scope, a suitable simulation code was developed in MATLAB and validated using the data available in literature. The results of the calculations show that temperature plays a crucial role in the anaerobic digestion process, since it strongly affects the kinetic rates of the microbial species and the methane production. The results obtained in terms of temperature fields and biogas production are compared with the ones available in literature, dealing with a continuously stirred tank reactor. The comparison is conducted considering that both reactors process a volumetric waste flow rate of 20 m^3/d and have the same structural characteristics. The plug flow reactor resulted better performance with a produced biogas flow rate equal to 2300 Nm^3/year.

Keywords: biogas production; mathematical modeling; thermal modeling; organic fraction of municipal solid waste

1. Introduction

The environmental impact of greenhouse gas (GHG) emissions on our planet are more alarming than ever [1]. The climate conditions of our planet are worsening from year to year, according to the IPCC annual reports [2]. Climate change also causes an increase in the energy demand [3] and the energy dependence of several countries [4]. The sharing of renewables in the energy context is thus mandatory [5]. Moreover, the issue of urban wastes disposal is also becoming increasingly important in the pathway of the energy transition [6]. The production of biogas allows the exploitation of renewable natural gas starting from wastes [7].

Biogas can be obtained by a plurality of different biomasses, which can differ in total solid content [8], alkalinity of the moisture [9], fats content [10], and other physicochemical characteristics [11]. This means that a well-organized structure for biomass harvesting in both urban and rural centers paves the way for a massive production of biogas [12]. The biogas may be used as a fuel for the cogeneration of combined heat and power (CHP) [13], which is the actual state of the art in biogas plant [14]. Otherwise, the biogas may be also upgraded into biomethane [15], separating CO_2 (and other impurities [16]) from CH_4 [17]. This biomethane can be used as fuel for vehicles [18] or injected into

the national gas grid [19]. The possibility of exploiting different biomasses leads to the necessity of considering different reactors in which the AD process occurs [20]. In fact, in case of manure, wastewater, or sewage sludges, up-flow anaerobic sludge blanket (UASB) reactors are used [21]. Conversely, in case of organic fraction of municipal solid waste (OFMSW), continuously stirred tank reactors (CSTR) or plug flow reactors (PFR) are mainly considered [22]. The fact that PFRs and CSTRs are more likely to be adopted in the case of OFMSW makes these technologies extremely attractive for the urban centers waste management [23].

Several works are available in literature presenting models for the biochemical behavior of the microbial species during the AD process [24]. In fact, mathematical modelling is crucial to correctly predict the biogas yield from the AD process [25]. The most diffused model adopted in case of low total solid content of the biomass is the ADM1 model, firstly developed by IWA task group [26]. The same authors of this work validated [27] and used this model in previous works to evaluate the production of biogas from the OFMSW in case of CSTRs [28]. However, in literature, some models are also available for the simulation of PFRs. A study on the modeling of the AD process in a PFR reactor was recently presented by Panaro et al. [29]. The model proposed in this work is based on second-order partial differential equations (PDEs) for the concentrations of the microbial species. Furthermore, the equations also consider the convective and diffusive phenomena that occur within the digester due to the concentration gradients. The computational domain is a 1D field in which the density is assumed constant. The model was used to predict the production of biogas from untreated manure bedded with straw and showed good results in terms of accuracy. This model is validated, also considering the variation of several pivotal parameters as the organic loading rate (OLR), hydraulic retention time (HRT), and length of the reactor. Veluchamy et al. [30] proposed a simple first-order reaction kinetic model for the substrate concentration and biogas yield variations along the PFR reactor. Further, in this case, the model is validated against experimental data collected in the laboratory. The reactor was a 65 L batch PFR operating with lignocellulosic corn-silage under mesophilic conditions. In this case, the maximum biogas yield of 0.264 m^3/kgVS d was obtained with the maximum OLR of 6.5 kg/m^3d and HRT of 17 days. An interesting model is proposed by Donoso-Bravo et al. [31], which assessed that a PFR can be studied as a chain of *n* CSTR connected in series, by means of mass balances. In this case, the output of the first reactor becomes the input of the second one, and so on until the *n*-th CSTR reactor is reached. The modified ADM1 is the biological model adopted for the prediction of the biogas production and results are validated by means of 160 L batch-scale reactor operating with cow manure. Several models were tested and compared to predict the biogas production in case of non-perfect mixing of digester. The PFR model results slightly overestimated the performance of the reactor with respect to other models based on nonideal mixing assumption.

Unfortunately, even the most accurate models for the biogas yield prediction in PFRs do not consider the thermal phenomena, which occur in these digesters, despite their relevance [32]. In [33], the authors performed a thermal analysis of a PFR by considering the thermal losses through the external walls and the solar radiative contribution. No models are considered for the AD process temperature due to the thermal inertia of the biomass within the reactor. Recently, in [34], the authors proposed an interesting analysis of the optimal control of the nonlinear dynamics of the reactants concentrations by means of the temperature. This parameter was regulated by means of an external heat exchanger, and the relevance of the temperature effect was assessed. However, in this case, a detailed coupling with the AD process was considered. In Wu et al. [35], a 3D model, based on first-order kinetic equations, mass and energy continuity, and species transport is presented. The numerical simulation is performed in Fluent 6.1 to predict the concentration distribution and temperature variation in the whole dominium. Comparison with experimental data available in literature showed an error below 5% with a temperature gradient lower than 5 K. The same authors [36] also investigated the heat transfer phenomena occurring between the external surface of the reactor and the environment. Several geometries, cylindrical and

rectangular, were proposed and the cylindrical one with a flat cover resulted the least heat dissipating. However, no study regarding heat transfer processes within the PFR reactor are available in literature.

Aim and Novelty of the Work

The aim of this work is to fill the gap in the scientific knowledge regarding the modeling of both biological and thermal phenomena that occur during the anaerobic digestion in PFRs. The literature review presented in this section showed that biological models are widely applied to PFRs. The relevance of the heat transfer contribution to the AD process is vastly recognized but accurate models for the prediction of the temperature gradients, strictly related to the biological ones, are still missing for these reactors. In particular, the available models are not coupled with accurate biological models and do not consider the thermal inertia of the input biomass and digester. These limitations are overcome in the present work and the novelties can be listed as follows:

- A detailed and comprehensive integrated thermal and biological model, also removing the common assumption of steady state, is considered. In particular, a detailed 1-D transient simulation model that couples both the biological and thermal aspects of the AD of OFMSW in a PFR is proposed.
- The thermal model considers the heat transfer between the OFMSW and the internal heat exchanger, in addition to the heat transfer between the reactor and the environment.
- The PFR model is compared to a CSTR one previously developed to assess how different reactors may influence biogas production, starting from the same input biomass.

Simulations are performed in MatLab® and results in terms of time-dependent biochemical species evolution and temperature variations are shown and discussed.

2. Method

A model able to simultaneously simulate the thermal and biological processes occurring within the reactor is implemented in MatLab®. The effectiveness of thermal exchange strictly depends on the geometrical and structural features of the digester and the design of the heating system. By means of the design of the heat exchange system, the temperature profile inside the digester can be predicted. This is a crucial step to determine one of the most significant parameters of the AD process. As mentioned before, the thermal model is strictly related to the biological one, since the biological kinetics are dramatically affected by the operating temperature. By means of this comprehensive model, it is possible to calculate the time histories of the temperature profiles and of the concentration profiles of the different substances and of the biogas flow rate.

In the following sections, the thermal and biological models are described in detail.

2.1. Biological Model

The ADM1 is the most widely recognized and popular mathematical model to describe the anaerobic digestion (AD) process [37]. As previously discussed, this model was extensively used and validated vs. experimental data in many studies. In this work, the simplified version of ADM1 [38] was implemented and a few processes and substrate components with respect to general model were considered [39].

Assuming that the input OFMSW flow rate is equal to the output digestate ($\dot{V}_{OFMSW,in} = \dot{V}_{digestate,out}$) and that the volume occupied by the waste remains constant, the mass balance equations of the model can be generalized as follows:

$$\frac{dC_{OFMSW,i}}{dt} = \frac{\dot{V}_{OFMSW}}{V_{OFMSW}}(C_{OFMSW,i,in} - C_{OFMSW,i}) + \sum_j \rho_j \nu_{i,j} \tag{1}$$

This equation represents the mass balance for the generic component *i*, and $C_{OFMSW,in}$ and $C_{OFMSW,i}$ are the input concentrations of *i*th component contained in the waste and the concentration of it in the reactor during the AD process, respectively. The last term

of Equation (1) is the sum of kinetics of reaction of jth process (ρ_j) multiplied by the biochemical coefficient of the ith component in the jth reaction ($\nu_{i,j}$).

The simplified ADM1 model consists of 13 differential mass balance equations, one for each organic matter component. In Table 1, the soluble substrates are indicated with S_i and the insoluble ones with X_i:

Table 1. Components of OFMSW.

X_C	Composite particulate organic matter
X_S	Simple particulate organic matter
X_I	Particulate inert
S_I	Soluble inert organic matter
S_{so}	Soluble organic matter
S_{oa}	Organic acid
S_{ac}	Acetate
S_{H2}	Hydrogen
S_{CH4}	Methane
X_{acid}	Acidogenic bacteria
X_{metaAC}	Acetoclastic methanogens bacteria
X_{acet}	Acetogenic bacteria
X_{metaH2}	Hydrogenotrophic methanogens bacteria

These concentrations are expressed in $kgCOD/m^3$ and evolve in different ways according to the active phase during the AD process. The reactions kinetics are considered by means of the last term of Equation (1), which differ for each component and process. Values are specified in Table 2.

Table 2. Kinetic terms for the different components of OFMSW.

X_C	$-k_{dis,T}X_C + k_{d,\ acid}\ X_{acid} + k_{d,\ acet}\ X_{acet} + k_{d,\ metaAC}\ X_{metaAC} + k_{d,\ metaH2}\ X_{metaH2}$
X_S	$f_{X_S,X_C}k_{dis,T}X_C - k_{idro,T}X_S$
X_I	$f_{X_i,X_C}k_{dis_T}X_C$
S_I	$f_{S_I,X_C}k_{dis_T}X_C$
S_{so}	$k_{idro,T}X_S - \nu_{acid,T}X_{acid}$
S_{oa}	$(1-Y_{acid})\nu_{acid,T}X_{acid} - \nu_{acet,T}X_{acet}$
S_{ac}	$f_{S_{ac},S_{oa}}(1-Y_{acet})\nu_{acet,T}X_{acet} - \nu_{\ metaAC,T}X_{\ metaAC}$
S_{H2}	$f_{S_{H2},S_{oa}}(1-Y_{acet})\nu_{acet,T}X_{acet} - \nu_{metaH2,T}X_{metaH2}$
S_{CH4}	$(1-Y_{metaAC})\nu_{\ metaAC,T}X_{\ metaAC} + (1-Y_{metaH2})\nu_{metaH2,T}X_{metaH2}$
X_{acid}	$Y_{acid}\nu_{acid,T}X_{acid} - k_{d,\ acid}\ X_{acid}$
X_{mataAC}	$Y_{acet}\nu_{acet,T}X_{acet} - k_{d,\ acet}\ X_{acet}$
X_{acet}	$Y_{metaAC}\nu_{metaAC,T}X_{metaAC} - k_{d,\ metaAC}\ X_{metaAC}$
X_{metaH2}	$Y_{metaH2}\nu_{metaH2,T}X_{metaH2} - k_{d,\ metaH2}X_{metaH2}$

where,

- $\nu_{acid,T} = \nu_{max,acid,T}\cdot\dfrac{S_S}{k_{s,\ acid}+S_S}$
- $\nu_{acet,T} = \nu_{max,acet,T}\cdot\dfrac{S_{oa}}{k_{s,\ acet}+S_{oa}}$
- $\nu_{metaAC,T} = \nu_{max,metaAC,T}\cdot\dfrac{S_{ac}}{k_{s,metaAC}+S_{ac}}$
- $\nu_{metaH2,T} = \nu_{max,metaH2,T}\cdot\dfrac{S_{H2}}{k_{s,metaH2}+S_{H2}}$

2.2. Thermal Model

The thermal model consists of two energy balance equations. They constitute a system of two equations in two variables: the output water temperature $T_{water,out}$ and the output digestate temperature $T_{digestate\ out}$.

The reactor can be represented by means of the following scheme in Figure 1:
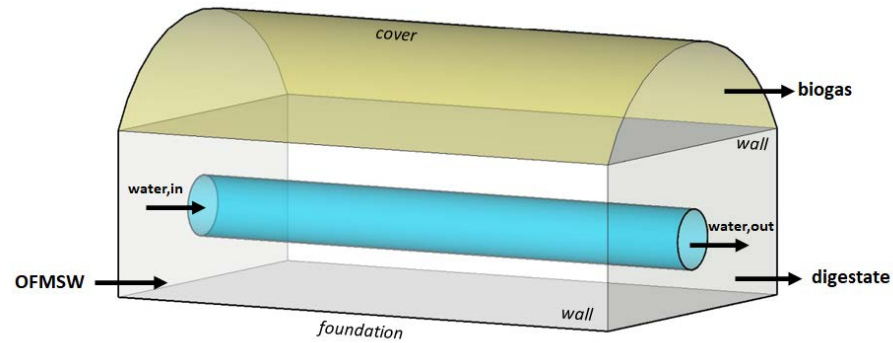

Figure 1. Sketch of the PFR.

The first equation is the energy balance equation of the digester:

$$\dot{m}_{water}c_{water}\left(T_{water,in} - T_{water,out}\right) + \dot{m}_{OFMSW}c_{p,OFMSW}T_{OFMSW,in} - \dot{m}_{digestate}c_{p,digestate}T_{digestate,out}$$
$$-\dot{m}_{biogas}c_{p,biogas}T_{digestate,out} - \dot{Q}_{dis} = \rho_{OFMSW}V_{OFMSW}c_{p,OFMSW}\frac{dT_{OFMSW}}{dt} \tag{2}$$

in which the biogas and digester temperature are assumed to be equal to the output OFMSW temperature.

The thermal flow rate loss of the digester is equal to

$$\dot{Q}_{dis} = \dot{Q}_{dis,cover} + \dot{Q}_{dis,walls} + \dot{Q}_{dis,foundation} \tag{3}$$

The three terms of Equation (3) are the thermal flow rate loss through the digester cover, lateral walls, and foundation, respectively. Assuming that the digester temperature is equal to the mean waste temperature $\overline{T_{OFMSW}}$, Equation (3) becomes

$$\dot{Q}_{dis} = U_{cover}A_{cover}\left(\overline{T_{OFMSW}} - T_{amb}\right) + U_{walls}A_{walls}\left(\overline{T_{OFMSW}} - T_{amb}\right)$$
$$+U_{foundation}A_{foundation}\left(\overline{T_{OFMSW}} - T_{ground}\right) \tag{4}$$

The global heat transmission coefficients U are calculated considering components and thermophysical parameters that will be discussed in the following section:

$$U = \frac{1}{\frac{1}{h_{int}} + \sum_{i=1}^{n}\frac{s_i}{\lambda_i} + \frac{1}{h_{est}}} \tag{5}$$

where $\sum_{i=1}^{n}\frac{s_i}{\lambda_i}$ is the sum of the conductive thermal resistances calculated as the ratio of the thickness of the various digester walls' layers s_i and their thermal conductivity λ_i. h_{int} is the convective coefficient between the digester walls' internal surface and the OFMSW, in the case of U_{walls} and $U_{foundation}$, or the biogas, in the case of U_{cover}. h_{est} is the convective coefficient between the digester walls external surface and the environment, in the case of U_{walls} and U_{cover}, or the ground, in the case of $U_{foundation}$.

For the calculation of U_{walls}, the convective heat exchange resistance along the internal digester walls was neglected since the OFMSW is a predominantly solid substrate. The digester foundation transmittance $U_{foundation}$ was calculated neglecting the convective thermal resistance that occurs along the surface in contact with the OFMSW and the ground.

An additional equation (to be coupled with Equation (2)) is required to complete the system of equations. This equation can be obtained by the energy balance on the reactor heat exchanger:

$$\dot{m}_{water} c_{p,water} (T_{water,in} - T_{water,out}) = n U_{HE,n} A_{HE,n} (\overline{T_{water}} - \overline{T_{OFMSW}}) \tag{6}$$

Neglecting the thermal resistance between OFMSW and tube walls and assuming constant the OFMSW temperature, $U_{HE,n}$ can be calculated as follows:

$$U_{HE,n} = \frac{1}{\frac{1}{h_{int,water}} + \frac{s_{HE}}{\lambda_{HE}}} \tag{7}$$

where the convection coefficient along the internal side of the pipe $h_{int,water}$ was calculated with the following equation [40]:

$$h_{int,water} = \frac{\lambda_{water}}{DN_{HE,n}} Nu \tag{8}$$

where $DN_{HE,n}$ is the pipe nominal diameter and Nu is the Nusselt number calculated with Dittus–Boelter correlation [40].

2.3. Thermal–Biological Model

Since the reactor considered is a PFR, the input substrate undergoes the anaerobic process while moving along the digester. Therefore, the components concentrations change in the flow direction, as well as in time. In the proposed model, Equations (1), (2) and (6) were discretized with respect to time and space.

In this way, in space, the digester was supposed to be constituted by several CSTRs connected in series [31], each by means of mass balances. The ADM1 model was solved for each CSTR where the output of the first one corresponds to the inlet conditions of the following one, and so on.

For the first time step, the input conditions were fixed according to the substrate characteristics entering the reactor. The value of C_p at the inlet of the reactor is assumed to be equal to the one of the OFMSW, whereas the output biomass is supposed to be digestate, with a different value of C_p. Both these values of specific heat are also assumed to be constant with the temperature since, in the PFR reactor, no relevant temperature gradients are expected. The inlet parameters of the biological model are summarized in Table 3 while the stoichiometric coefficients, kinetic parameters, and rates have been assumed equal to the ones reported in a previous work of the authors (Table 4 in [27]).

Table 3. Inlet parameters of the model.

	Value	*Unit*
ρ_{OFMSW}	750	kg/m^3
$c_{p,OFMSW}$	2.72	
$c_{p,digestate}$	4.18	kJ/(kg K)
$c_{p,biogas}$	1.42	
$X_{C,in}$	300	
$X_{acid,in} - X_{acet,in} - X_{metaAc,in} - X_{meta\ H2,in}$	0.001	kgCOD/m^3
$T_{OFMSW,in} - T_{amb} - T_{ground}$	15	°C
$T_{water,in}$	55	
$\dot{m}_{OFMSW}$	0.174	kg/s
$\dot{m}_{water}$	0.756	

Table 4. Structural and thermal parameters of digester walls and foundation.

	Value		Unit
	Walls	*Foundation*	
s_{CONC}	0.2	0.4	
s_{XPS-SL}		0.1	
s_{ST}	0.005	-	m
$s_{CLS,2}$	-	0.5	
λ_{CLS}		2.3	
λ_{XPS-SL}		0.036	W/(m K)
λ_{MG}	-	1.6	

Assuming that the digester is in thermodynamic equilibrium with the ambient before the heating, the ambient temperature is assumed as an initial condition for the biomass. The biogas flow rate and the digestate flow rate—the latter calculated as the difference between biomass and biogas flow rates—are obtained from the biological model. Once the flow rates are known, the waste temperature can be obtained by means of the digester thermal balance and the water temperature by the HE thermal balance.

For the following time steps, the procedure is repeated but the input substrate characteristics of each CSTR will correspond to the output ones by the same in the preceding dt.

3. Case Study

3.1. Reactor Structural and Thermal Parameters

The digester is featured by a parallelepiped shape and is equipped with walls in concrete and a polystyrene insulation layer (XPS-LS). The lateral walls are covered with a stainless steel corrugated sheet, while the inferior bottom with another concrete layer. In Table 4, the thickness and thermal parameters of each layer are shown.

$s_{CONC}s_{XPS-SL}s_{ST}s_{CLS,2}\lambda_{CLS}\lambda_{XPS-SL}\lambda_{MG}$ A gasometric dome, consisting of two PVC membranes separated by an air-filled cavity, covers the reactor. The internal one may vary its volume depending on the amount of biogas accumulated below. The external one is stiff, so it is necessary to add or extract air from cavity to keep the pressure level within the reactor utmost constant. The gasometric dome structural and thermal parameters are summarized in Table 5, where R_{air} is the resistance in the air gap between the two membranes.

Table 5. Gasometric dome structural and thermal parameters.

	Value	Unit
S_{PVC}	0.001	m
$h_{int,biogas}$	10	W(m^2 K)
R_{air}	0.13	(m^2 K)/W

The membranes' thermal resistance is negligible because they are thin and consist of plastic material with relatively high thermal conductivity.

The reactor is designed for a hydraulic retention time (HRT) of 30 days and a volumetric waste flow rate $\dot{V}_{OFMSW}$ of 20 m^3/d. The cross-sectional dimension of the reactor, $A_{reactor}$, is determined with a height of 4 m and base equal to 10 m. Thus, the length L can be calculated as follows:

$$L = \frac{\dot{V}_{OFMSW} \cdot HRT}{A_{reactor}} \tag{9}$$

The total reactor volume, equal to 840 m^3, has been calculated considering that it is filled $\frac{3}{4}$ with waste and the remaining part consists of the volume underlying the dome.

3.2. Heating System

The system used to heat the digester consists of high-density cross-linked polyethylene (PE-Xa) pipes operating in parallel-flow.

The AD process occurs in mesophilic conditions, at a temperature between 35 and 40 °C. Assuming a digester operating temperature equal to 40 °C, the thermal flow rate that must be supplied to the reactor is evaluated as follows:

$$\dot{Q}_{reactor} = \dot{Q}_{OFMSW} + \dot{Q}_{diss} \tag{10}$$

$$\dot{Q}_{OFMSW} = \dot{m}_{OFMSW} c_{p,OFMSW} \left(T_{digester} - T_{OFMSW,in} \right) \tag{11}$$

where $\dot{Q}_{OFMSW}$ is the heat transfer rate supplied to the OFMSW. $c_{p,OFMSW} = 2.72 \text{kJ}/(\text{kg K})$ and $\dot{m}_{OFMSW} = 0.174 \text{ kg/s}$ are, respectively, the specific heat and the mass flow rate of OFMSW. $T_{OFMSW,in}$ is the inlet waste temperature assumed equal to the ambient temperature $T_{amb} = 15$ °C.

Given the pipe diameter and assuming that each pipe is featured by the same length of the digester, a suitable number of pipes included into the heat exchanger can be selected so that $\dot{Q}_{reactor}$ is equal to the thermal flow rate of the hot water $\dot{Q}_{water}$:

$$\dot{Q}_{water} = n U_{HE,n} A_{HE,n} \Delta T_{lm} \tag{12}$$

where log-mean temperature can be calculated as follows [40]:

$$\Delta T_{lm} = \frac{\left(T_{water,in} - T_{digester} \right) - \left(T_{water,out} - T_{digester} \right)}{\ln\left(\frac{T_{water,in} - T_{digester}}{T_{water,out} - T_{digester}} \right)} \tag{13}$$

In Table 6, the heat exchanger structural and thermal parameters are reported.

Table 6. HE structural and thermal parameters.

	Value	*Unit*
s_{PE-Xa}	0.0018	m
$DN_{HE,n}$	0.025	
λ_{PE-Xa}	0.38	W/(m K)
λ_{water}	0.65	
ρ_{water}	987.70	kg/m^3
c_{water}	4.178	kJ/(kg K)
Pr	3.65	
Re	9586	
Nu	51.97	
$T_{water,in}$	55	°C
$T_{water,out}$	45	

4. Results

The simulation was carried out for a time span of 60 days, using a time step of 1.5 min and a mesh with spacing of 0.1 m.

Figure 2 reports the trend of output OFMSW and output water temperature in two different simulation times: Figure 2a shows the 1-D temperature profile along the reactor at $t = 1.5$ min, while Figure 2b shows the same temperatures after 12 days. Note that the trend reported in Figure 2 represents a stationary condition achieved by the digester. In other words, after 12 days, the 1-D temperature profile does not change as a function of time. As expected at 1.5 min, the OFMSW temperature is almost constant along the reactor since the thermal inertia of the mass included in the digester is so high that it takes a long time to heat the mass included in the system. Conversely, at 12 days, a nonmonotonic trend is detected. This is due to the fact that in the first part of the reactor, the temperature of OFMSW sharply increases due to internal heat exchanger. Then, a slight decrease in the OFMSW temperature is detected due to the parallel flow configuration of the heat exchanger, determining a decreasing trend in the temperature of the hot water.
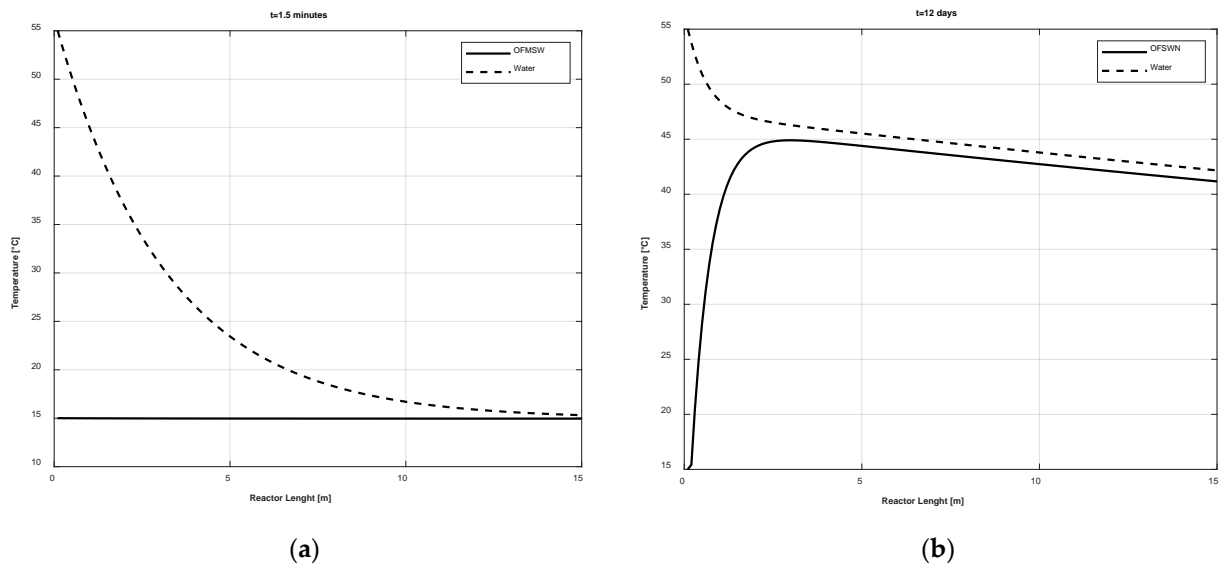
(**a**)   (**b**)

Figure 2. Output OFMSW and output water temperature at t = 1.5 min (**a**) and t = 12 days (**b**).

The total flow rate of biogas is estimated assuming that the biogas mixture includes 65% of CH_4 and 35% of CO_2. Figure 3 shows the trend of the concentration of the methane at the last slice of 1-D discretization of the PFR. The double exponential trend is due to two bacteria families responsible for the production of methane.
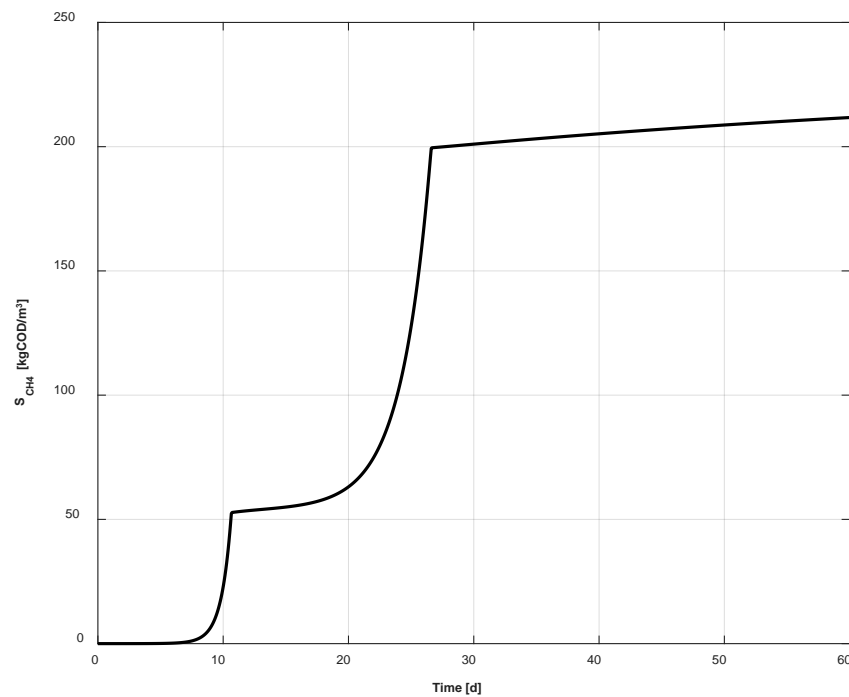

Figure 3. Concentration of CH_4 at the end of PFR.

Figure 4 proves that the hydrogenotrophic methanogenesis firstly occurs. In fact, hydrogen begins to rapidly decrease after 10 days (S_{H2}, Figure 4), when the biomethane production exhibits an exponential trend (S_{CH4}, Figure 4). The second exponential trend is linked to acetate consumption, which is much more consistent in terms of quantity. This process ends after roughly 25 days of process, after which the waste is stabilized and biomethane production stops.
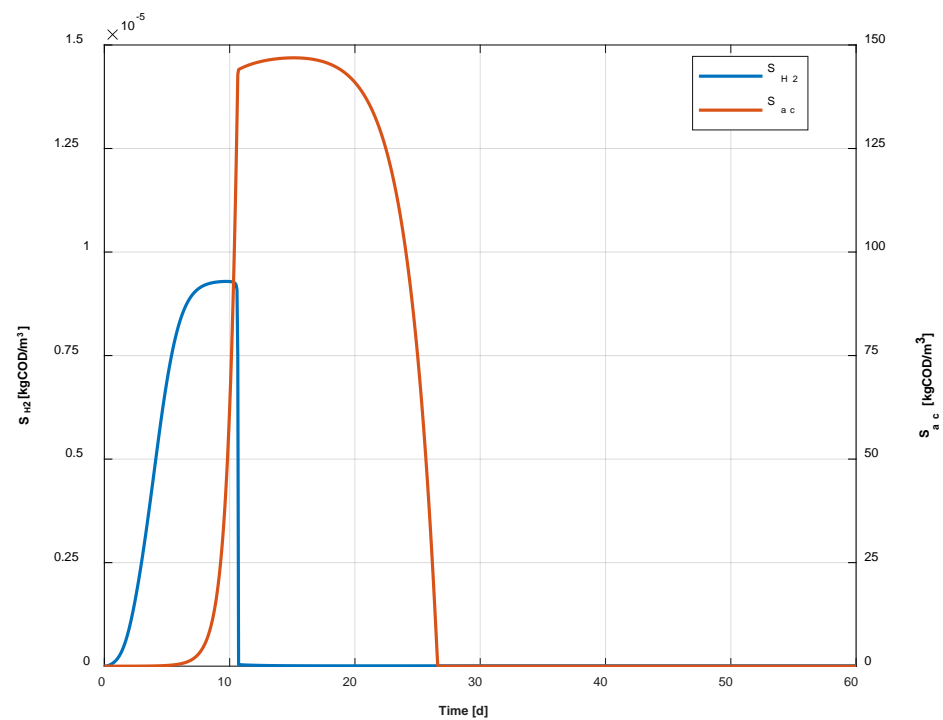
Figure 4. Concentration of H_2 and acetate at the end of PRF.

The biogas produced, shown in Figure 5, follows, as expected, the trend of S_{CH4}.
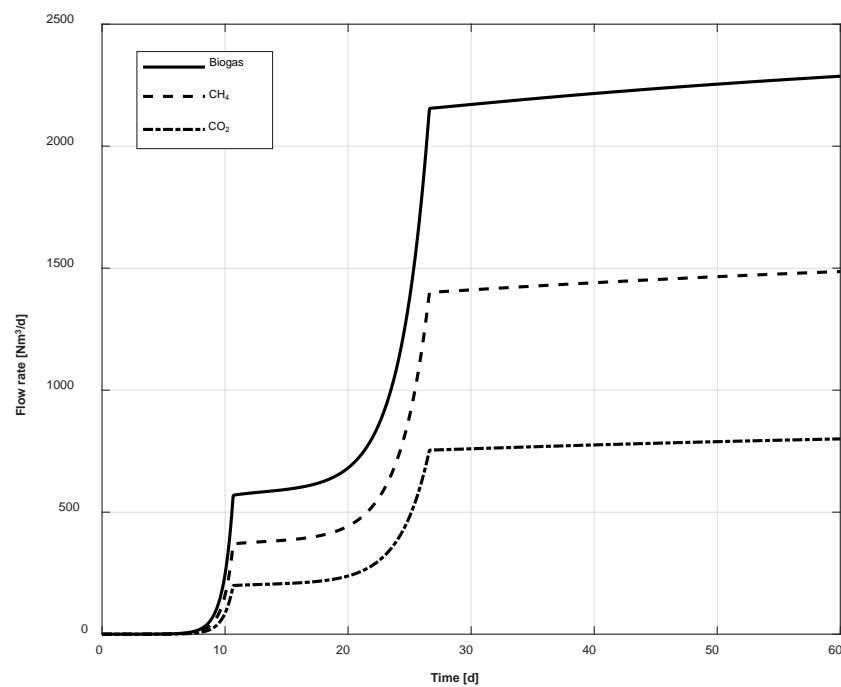

Figure 5. Biogas, CH_4, and CO_2 flow rate at the end of PFR.

Biogas production along the PFR is roughly constant, as shown in Figure 6a. For advanced slices of PFR, the beginning of the biomethane production and of the exponential phase is forwardly shifted from the time point of view. The output waste temperature, which varies from slice to slice in the PFR, is one of the most important parameters of the biological model, affecting the metabolic activity of bacteria into the digester. The higher the temperature, the faster the development of the biological model, see Figure 6a,b.
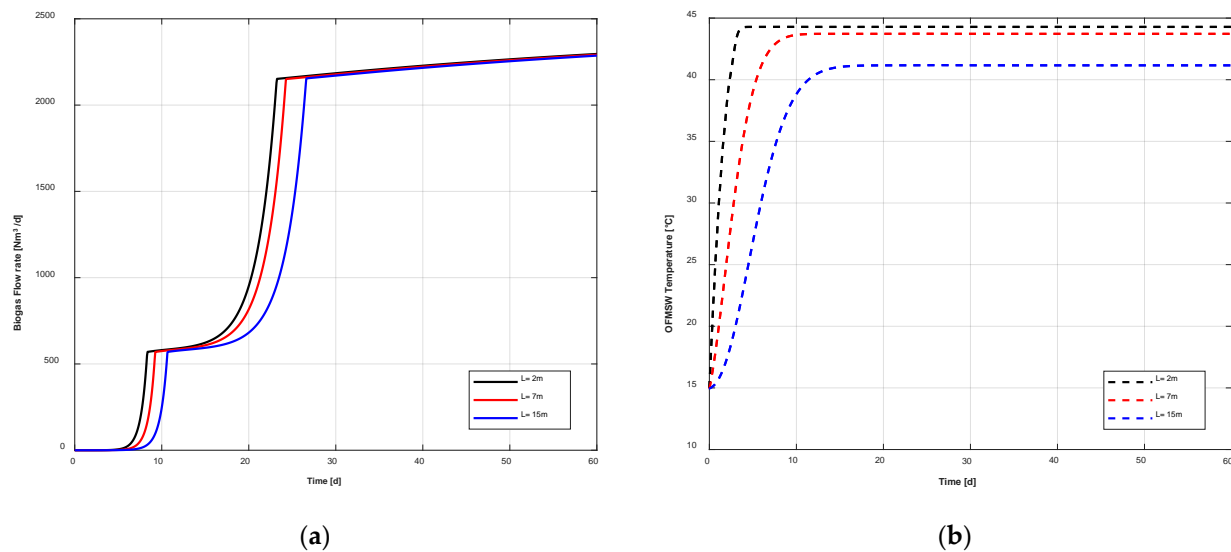
(**a**)   (**b**)

Figure 6. Volumetric biogas flow rate (**a**) and output OFMSW Temperature (**b**) in different positions of the PFR.

The exponential trend begin is timely shifted considering adjacent digester slices, i.e., computational nodes, the start of the exponential trend is delayed for the computational node located in advance (Figure 6a). This trend is due to the fact that the temperature rises more rapidly for the inlet nodes, with respect to the advanced nodes. For example, at 2 m from the PFR inlet, the digester temperature is always greater than the one at 15 m (Figure 6b) from the inlet. In fact, the higher the digester temperature—in the mesophilic temperature range—the faster the biological processes.

Finally, the proposed PFR model is compared with the CSTR model [27], see Figure 7. These two digesters are featured by the same structural characteristics and they process the same waste flow rate. The biogas flow rate production in PFR is higher than one in the CSTR, as shown in Figure 6.
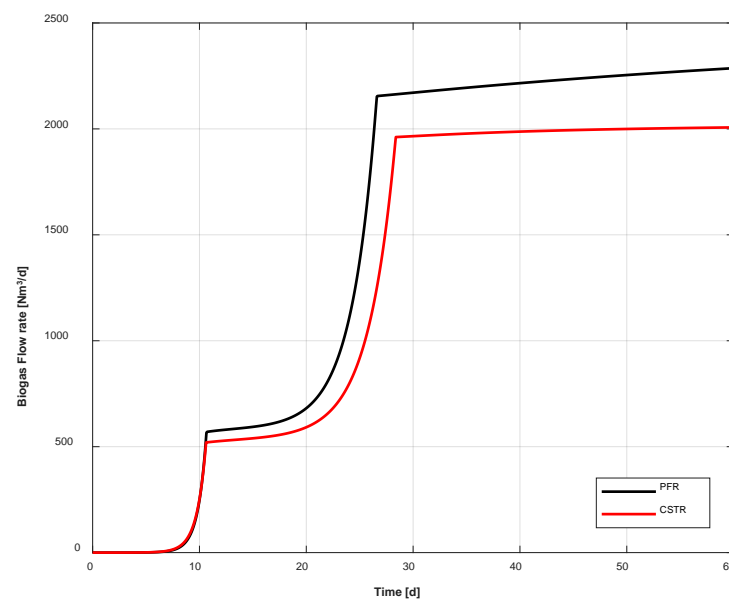

Figure 7. Comparison between the biogas flow rate in PFR and CSTR.

This result is mainly due to the higher slope of the temperature curve in the case of PFR, which leads to a greater amount of biogas produced in the methanogenic phase

(Figure 7). In fact, as mentioned before, the higher the digester temperature, the faster the biological processes. In addition, a higher temperature promotes the biogas production by the bacteria.

To support this result, the OFMSW temperature and the heat transfer rate involved for both the reactors were analyzed and compared. In Figure 8, the trend of the heat transfer rate within the reactor and the thermal losses are reported, both for the CSTR (Figure 8a) and the PFR (Figure 8b).
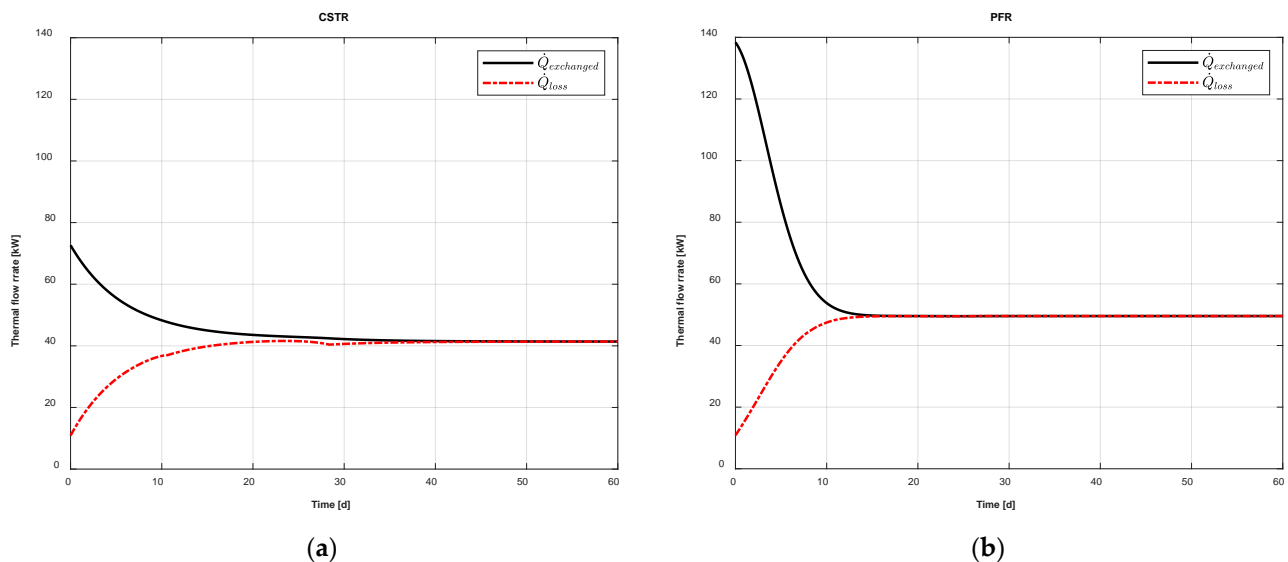

(**a**) (**b**)

Figure 8. Exchanged and loss thermal flow rate in CSTR (**a**) and in PFR (**b**).

The exchanged thermal flow rate, $\dot{Q}_{exchanged}$, represents the total input energy. This term represents the thermal energy supplied to the digester by means of the heat exchanger installed into the digester. The thermal losses, $\dot{Q}_{loss}$, are due to the heat loss toward the environment and the thermal flow rate related to the outgoing biogas and digestate.

Figure 8 proves that the PFR model is featured by a lower thermal inertia with respect to the CSTR one. In fact, the heat exchanger supplies a higher amount of heat to the waste into the digester in the PFR model with respect to the CSTR case. In addition, PFR achieves the steady state earlier, i.e., 12 days (PFR) vs. 22 days (CSTR). Figure 9 compares the temperatures of the CSTR and PFR.
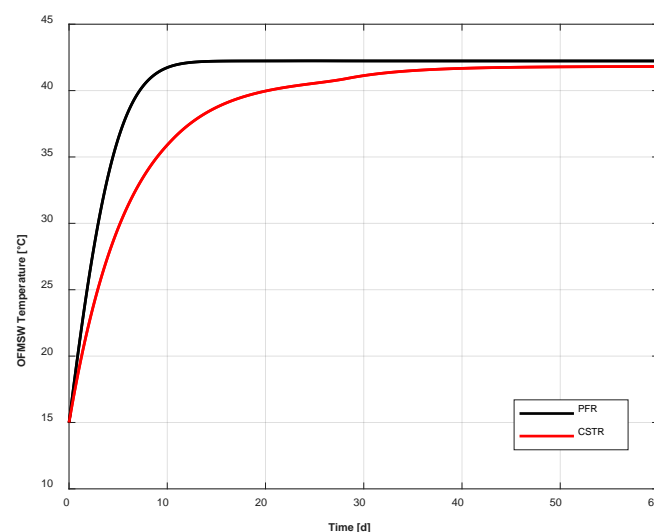

Figure 9. Comparison between the OFMSW Temperature in PFR and CSTR.

Note that, concerning the PFR, this figure reports the average temperature among all the computational nodes of the PFR. This figure is consistent with the heat transfer rate trends discussed before. Since the lower thermal inertia of the PFR determines a higher amount of heat supplied to the waste. Therefore, PFR temperature exhibits a sharp increase up to the steady state condition. Conversely, the CSTR achieves the steady state later with respect to the PFR. CSTR is also featured by a slightly lower operating temperature with respect to the PFR. This issue leads to the fact that the PFR is featured by higher thermal losses with respect to the CSTR: $\dot{Q}_{loss}$ is equal to 40 kW and 50 kW in steady state conditions for CSTR and PFR, respectively. However, the geometry of the studied digesters also affects the thermal losses. In fact, although both the digesters are featured by the same volume, CSTR is characterized by a compact shape, whereas PRF is characterized by a greater dispersing surface.

5. Conclusions

In this work, a one-dimensional model able to simulate the biological processes and the heat exchange occurring inside a plug flow reactor is proposed. The anaerobic digestion model is based on the well-known anaerobic digestion model n.1, widely adopted and validated in literature, and is coupled with the thermal balance equation regarding the heat exchanger installed into the digester envelope. With respect to the continuously stirred tank reactor, which considers a single temperature node, the plug flow reactor model also evaluates the temperature gradient along the digester. The model proposed consists in a set of partial differential equations, which are discretized with respect to space and time. Results are compared with the ones previously obtained for a continuously stirred tank reactor to further assess the consistency of the model.

The main findings from the comparison of the results obtained for both models can be summarized as follows:

- The considered digester achieves a biogas flow rate of 2300 Nm^3/d, which is slightly greater than the one obtained from the previous model.
- As expected, the temperature strongly affects the kinetic rates of the microbial species and the methane production. The faster the temperature increase, the faster the evolution of the biological process, for each slice of the reactor.
- The biogas production of the plug flow reactor is greater than the one in the continuously stirred tank reactor. This result is due to the fact that the average temperature along the plug flow reactor is greater than the temperature of the continuously stirred tank reactor, per each time step.

The reason of this temperature difference is mainly due to the greater thermal inertia of the continuously stirred tank reactor with respect to the plug flow reactor. Further development of this model may consider the integration of the proposed model for a plug flow reactor with a more complex system, including different renewable technologies, aiming at evaluating the dynamic renewable driven plant producing biogas.

Nomenclature

$Y_{substrate}$	Yield of biomass on substrate
$k_{d,substrate}$	First-order decay rate of substrate
$k_{dis,T}$	Disintegration reaction rate at temperature T
$k_{idro,T}$	Hydrolysis reaction rate at temperature T
$f_{product,substrate}$	Yield of product on substrate
$v_{max,substrate,T}$	Substate reaction rate at temperature T
$k_{s,process}$	Half-saturation constant of process

References

1. Baskin, C.C. Chapter 16—Effects of climate change on annual crops: The case of maize production in Africa. In *Plant Regeneration from Seeds*; Baskin, C.C., Baskin, J.M., Eds.; Academic Press: Cambridge, MA, USA, 2022; pp. 213–228. [CrossRef]
2. Johansen, K.; Werner, S. Something is sustainable in the state of Denmark: A review of the Danish district heating sector. *Renew. Sustain. Energy Rev.* **2022**, *158*, 112117. [CrossRef]
3. IEA. Climate Change. Available online: https://www.iea.org/topics/climate-change (accessed on 15 May 2022).
4. Deutch, P.J. Energy Independence. *Foreign Policy* **2005**, *151*, 20–25.
5. Antonelli, M.; Desideri, U.; Franco, A. Effects of large scale penetration of renewables: The Italian case in the years 2008–2015. *Renew. Sustain. Energy Rev.* **2018**, *81*, 3090–3100. [CrossRef]
6. Tang, Y.-T.; Huang, C. Disposal of Urban Wastes. In *Encyclopedia of Sustainable Technologies*; Abraham, M.A., Ed.; Elsevier: Oxford, UK, 2017; pp. 365–377. [CrossRef]
7. Obaideen, K.; Abdelkareem, M.A.; Wilberforce, T.; Elsaid, K.; Sayed, E.T.; Maghrabie, H.M.; Olabi, A.G. Biogas role in achievement of the sustainable development goals: Evaluation, Challenges, and Guidelines. *J. Taiwan Inst. Chem. Eng.* **2022**, *131*, 104207. [CrossRef]
8. Xu, F.; Wang, Z.-W.; Tang, L.; Li, Y. A mass diffusion-based interpretation of the effect of total solids content on solid-state anaerobic digestion of cellulosic biomass. *Bioresour. Technol.* **2014**, *167*, 178–185. [CrossRef]
9. Yu, J.; Guo, Q.; Gong, Y.; Ding, L.; Wang, J.; Yu, G. A review of the effects of alkali and alkaline earth metal species on biomass gasification. *Fuel Process. Technol.* **2021**, *214*, 106723. [CrossRef]
10. Neves, V.T.d.C.; Sales, E.A.; Perelo, L.W. Influence of lipid extraction methods as pre-treatment of microalgal biomass for biogas production. *Renew. Sustain. Energy Rev.* **2016**, *59*, 160–165. [CrossRef]
11. Kasinath, A.; Fudala-Ksiazek, S.; Szopinska, M.; Bylinski, H.; Artichowicz, W.; Remiszewska-Skwarek, A.; Luczkiewicz, A. Biomass in biogas production: Pretreatment and codigestion. *Renew. Sustain. Energy Rev.* **2021**, *150*, 111509. [CrossRef]
12. Xu, J.; Liu, Z.; Dai, J. Environmental and economic trade-off-based approaches towards urban household waste and crop straw disposal for biogas power generation project—A case study from China. *J. Clean. Prod.* **2021**, *319*, 128620. [CrossRef]
13. Dalpaz, R.; Konrad, O.; Cândido da Silva Cyrne, C.; Panis Barzotto, H.; Hasan, C.; Guerini Filho, M. Using biogas for energy cogeneration: An analysis of electric and thermal energy generation from agro-industrial waste. *Sustain. Energy Technol. Assess.* **2020**, *40*, 100774. [CrossRef]
14. Tricase, C.; Lombardi, M. State of the art and prospects of Italian biogas production from animal sewage: Technical-economic considerations. *Renew. Energy* **2009**, *34*, 477–485. [CrossRef]
15. Golmakani, A.; Ali Nabavi, S.; Wadi, B.; Manovic, V. Advances, challenges, and perspectives of biogas cleaning, upgrading, and utilisation. *Fuel* **2022**, *317*, 123085. [CrossRef]
16. Zhang, Y.; Kawasaki, Y.; Oshita, K.; Takaoka, M.; Minami, D.; Inoue, G.; Tanaka, T. Economic assessment of biogas purification systems for removal of both H2S and siloxane from biogas. *Renew. Energy* **2021**, *168*, 119–130. [CrossRef]
17. Wu, L.; Wei, W.; Song, L.; Woźniak-Karczewska, M.; Chrzanowski, Ł.; Ni, B.-J. Upgrading biogas produced in anaerobic digestion: Biological removal and bioconversion of CO_2 in biogas. *Renew. Sustain. Energy Rev.* **2021**, *150*, 111448. [CrossRef]
18. Singh, P.; Kalamdhad, A.S. Biomethane plants based on municipal solid waste and wastewater and its impact on vehicle sector in India—An Environmental-economic-resource assessment. *Environ. Technol. Innov.* **2022**, *26*, 102330. [CrossRef]
19. Cucchiella, F.; D'Adamo, I.; Gastaldi, M.; Miliacca, M. A profitability analysis of small-scale plants for biomethane injection into the gas grid. *J. Clean. Prod.* **2018**, *184*, 179–187. [CrossRef]
20. Calise, F.; Cappiello, F.L.; Cimmino, L.; d'Accadia, M.D.; Vicidomini, M. A Review of the State of the Art of Biomethane Production: Recent Advancements and Integration of Renewable Energies. *Energies* **2021**, *14*, 4895. [CrossRef]
21. Cecconet, D.; Mainardis, M.; Callegari, A.; Capodaglio, A.G. Psychrophilic treatment of municipal wastewater with a combined UASB/ASD system, and perspectives for improving urban WWTP sustainability. *Chemosphere* **2022**, *297*, 134228. [CrossRef] [PubMed]
22. Rossi, E.; Pecorini, I.; Paoli, P.; Iannelli, R. Plug-flow reactor for volatile fatty acid production from the organic fraction of municipal solid waste: Influence of organic loading rate. *J. Environ. Chem. Eng.* **2022**, *10*, 106963. [CrossRef]
23. Curry, N.; Pillay, P. Biogas prediction and design of a food waste to energy system for the urban environment. *Renew. Energy* **2012**, *41*, 200–209. [CrossRef]

24. Weinrich, S.; Nelles, M. Systematic simplification of the Anaerobic Digestion Model No. 1 (ADM1)—Model development and stoichiometric analysis. *Bioresour. Technol.* **2021**, *333*, 125124. [CrossRef] [PubMed]

25. Kunatsa, T.; Xia, X. A review on anaerobic digestion with focus on the role of biomass co-digestion, modelling and optimisation on biogas production and enhancement. *Bioresour. Technol.* **2022**, *344*, 126311. [CrossRef] [PubMed]

26. Batstone, D.J.; Keller, J.; Vavilin, V. Anaerobic Digestion Model No. 1. *Water Sci. Technol.* **2002**, *45*, 65–73. [CrossRef] [PubMed]

27. Calise, F.; Cappiello, F.L.; Dentice d'Accadia, M.; Infante, A.; Vicidomini, M. Modeling of the Anaerobic Digestion of Organic Wastes: Integration of Heat Transfer and Biochemical Aspects. *Energies* **2020**, *13*, 2702. [CrossRef]

28. Calise, F.; Cappiello, F.L.; Dentice d'Accadia, M.; Vicidomini, M. Concentrating photovoltaic/thermal collectors coupled with an anaerobic digestion process: Dynamic simulation and energy and economic analysis. *J. Clean. Prod.* **2021**, *311*, 127363. [CrossRef]

29. Panaro, D.B.; Mattei, M.R.; Esposito, G.; Steyer, J.P.; Capone, F.; Frunzo, L. A modelling and simulation study of anaerobic digestion in plug-flow reactors. *Commun. Nonlinear Sci. Numer. Simul.* **2022**, *105*, 106062. [CrossRef]

30. Veluchamy, C.; Kalamdhad, A.S.; Gilroyed, B.H. Evaluating and modelling of plug flow reactor digesting lignocellulosic corn silage. *Fuel* **2021**, *287*, 119498. [CrossRef]

31. Donoso-Bravo, A.; Sadino-Riquelme, C.; Gómez, D.; Segura, C.; Valdebenito, E.; Hansen, F. Modelling of an anaerobic plug-flow reactor. Process analysis and evaluation approaches with non-ideal mixing considerations. *Bioresour. Technol.* **2018**, *260*, 95–104. [CrossRef] [PubMed]

32. Nie, E.; He, P.; Zhang, H.; Hao, L.; Shao, L.; Lü, F. How does temperature regulate anaerobic digestion? *Renew. Sustain. Energy Rev.* **2021**, *150*, 111453. [CrossRef]

33. Gebremedhin, K.G.; Wu, B.; Gooch, C.; Wright, P.; Inglis, S. Heat transfer model for plug-flow anaerobic digesters. *Trans. ASAE* **2005**, *48*, 777–785. [CrossRef]

34. Hastir, A.; Lamoline, F. Optimal equilibrium stabilization for a nonlinear infinite-dimensional plug-flow reactor model. *Automatica* **2021**, *130*, 109722. [CrossRef]

35. Wu, B.; Bibeau, E.L.; Gebremedhin, K.G. Three-Dimensional Numerical Simulation Model of Biogas Production for Anaerobic Digesters. In *2006 ASAE Annual Meeting*; American Society of Agricultural and Biological Engineers: St. Joseph, MI, USA, 2006.

36. Wu, B.; Bibeau, E.L. Development of 3-D anaerobic digester heat transfer model for cold weather applications. *Trans. ASABE* **2006**, *49*, 749–757. [CrossRef]

37. Batstone, D.; Puyol, D.; Flores-Alsina, X.; Rodríguez, R.J. Mathematical modelling of anaerobic digestion processes: Applications and future needs. *Rev. Environ. Sci. Biotechnol.* **2015**, *14*, 595–613. [CrossRef]

38. Liotta, F.; Chatellier, P.; Esposito, G.; Fabbricino, M.; Frunzo, L.; van Hullebusch, E.D.; Lens, P.N.L.; Pirozzi, F. Modified Anaerobic Digestion Model No.1 for dry and semi-dry anaerobic digestion of solid organic waste. *Environ. Technol.* **2015**, *36*, 870–880. [CrossRef] [PubMed]

39. Batstone, D.; Keller, J.; Angelidaki, I.; Kalyuzhnyi, S.; Pavlostathis, S.; Rozzi, A.; Sanders, W.; Siegrist, H.; Vavilin, V. Anaerobic digestion model No 1 (ADM1). *Water Sci. Technol.* **2002**, *45*, 65–73. [CrossRef]

40. Incropera, F.P. *Fundamentals of Heat and Mass Transfer*; John Wiley & Sons, Inc.: Hoboken, NJ, USA, 2006.